Title
Macrocytic Anemia and Mitochondriopathy Resulting from a Defect in Sideroflexin 4

Journal
American Journal of Human Genetics, 93(5)

ISSN
0002-9297

Authors
Hildick-Smith, Gordon J
Cooney, Jeffrey D
Garone, Caterina
et al.

Publication Date
2013-11-01

DOI
10.1016/j.ajhg.2013.09.011

Peer reviewed

REPORT

Macrocytic Anemia and Mitochondriopathy Resulting from a Defect in Sideroflexin 4

Gordon J. Hildick-Smith,[1,15,16] Jeffrey D. Cooney,[1,15,17] Caterina Garone,[2,15] Laura S. Kremer,[3,4] Tobias B. Haack,[3,4] Jonathan N. Thon,[1] Non Miyata,[5] Daniel S. Lieber,[6,7] Sarah E. Calvo,[6,7] H. Orhan Akman,[2] Yvette Y. Yien,[1] Nicholas C. Huston,[1] Diana S. Branco,[1,18] Dhvanit I. Shah,[1] Matthew L. Freedman,[8] Carla M. Koehler,[5] Joseph E. Italiano, Jr.,[1] Andreas Merkenschlager,[9] Skadi Beblo,[10] Tim M. Strom,[3,4] Thomas Meitinger,[3,4] Peter Freisinger,[11] M. Alice Donati,[12] Holger Prokisch,[3,4] Vamsi K. Mootha,[6,7] Salvatore DiMauro,[2] and Barry H. Paw[1,13,14,*]

We used exome sequencing to identify mutations in sideroflexin 4 (*SFXN4*) in two children with mitochondrial disease (the more severe case also presented with macrocytic anemia). SFXN4 is an uncharacterized mitochondrial protein that localizes to the mitochondrial inner membrane. *sfxn4* knockdown in zebrafish recapitulated the mitochondrial respiratory defect observed in both individuals and the macrocytic anemia with megaloblastic features of the more severe case. In vitro and in vivo complementation studies with fibroblasts from the affected individuals and zebrafish demonstrated the requirement of *SFXN4* for mitochondrial respiratory homeostasis and erythropoiesis. Our findings establish mutations in *SFXN4* as a cause of mitochondriopathy and macrocytic anemia.

Mitochondrial disorders are a group of diseases that affect 1 in 5,000 live births. Affected individuals can present at any age with a constellation of symptoms, such as failure to thrive, lactic acidosis, skeletal myopathy, deafness, blindness, other neurological defects, and impaired hematopoiesis. The genes underlying many hereditary forms of respiratory-chain disorders remain uncharacterized.[1] In contrast to those of mitochondriopathies, the etiologies of macrocytic anemia are better defined. However, in the first, more severe case, we excluded all known causes of macrocytosis.[2]

Here, we describe two individuals with mitochondriopathies. The first individual presented at birth with macrocytic erythroid abnormalities and mitochondrial disease. Subsequently, we identified a second individual with a milder mitochondriopathy and defects in the same gene. Individual 1, the more severe case, is a 14-year-old girl of European origin and was born to nonconsanguineous healthy parents in Italy. As a result of intrauterine growth retardation (IUGR) and oligohydramnios, delivery was induced at 37 weeks of gestation. At 48 hr of life, she had increased blood lactate (168 mg/dl; normal range = 10–60 mg/dl), ammonia (125 μg/dl; normal range = 12–55 μg/dl), and uric acid. A muscle biopsy showed mildly increased numbers of mitochondria and lipid droplets, whereas her brain MRI was normal. The infant's weight at birth was in the third percentile (2.25 kg); her length and cranial circumference also measured lower than the third percentile from birth to the age of 12 years. By 3 months of life, she suffered from macrocytic anemia. One year later, a repeat muscle biopsy revealed severe deficiency of mitochondrial complex I activity, which persisted until she reached 4 years of age (Table S1, available online). Global defects in respiratory-chain activity (RCA) were determined later in life in primary fibroblasts from individual 1 (Figures 1A–1C).[3] Since then, she has gradually improved but remains dysmorphic and underweight (less than the third percentile) with atrophic muscles and difficulty running. Additional neurological symptoms include tremor, dysmetria, language delay, and mild intellectual disability. Despite a normal retinogram, she has a severe visual deficit. When she was 13 years of age, her red blood cells retained macrocytic indices (Table S2) with hypersegmented neutrophils (Figure 1D). Since she was 3 years of age, her diet has been supplemented with carnitine, coenzyme Q_{10}, and vitamins C and B_1.

[1]Division of Hematology, Department of Medicine, Brigham and Women's Hospital and Harvard Medical School, Boston, MA 02115, USA; [2]Department of Neurology, Columbia University Medical Center, New York, NY 10032, USA; [3]Institute of Human Genetics, Technische Universität München, 80333 Munich, Germany; [4]Institute of Human Genetics, Helmholtz Zentrum München, 85764 Neuherberg, Germany; [5]Department of Chemistry and Biochemistry, University of California, Los Angeles, Los Angeles, CA 90095, USA; [6]Departments of Molecular Biology and Medicine, Massachusetts General Hospital and Harvard Medical School, Boston, MA 02114, USA; [7]Department of Systems Biology, Harvard Medical School, Boston, MA 02115, USA; [8]Department of Medical Oncology, Dana-Farber Cancer Institute and Harvard Medical School, Boston, MA 02115, USA; [9]Department of Neuropediatrics, University Hospital for Children and Adolescents, University of Leipzig, 04103 Leipzig, Germany; [10]Department of Inborn Metabolic Diseases, University Hospital for Children and Adolescents, University of Leipzig, 04103 Leipzig, Germany; [11]Department of Pediatrics, Kinderklinik Klinikum Reutlingen, 72764 Reutlingen, Germany; [12]Unit of Metabolic and Muscular Diseases, Meyer Children Hospital, 50132 Florence, Italy; [13]Division of Hematology-Oncology, Department of Medicine, Boston Children's Hospital and Harvard Medical School, Boston, MA 02115, USA; [14]Department of Pediatric Oncology, Dana-Farber Cancer Institute and Harvard Medical School, Boston, MA 02115, USA
[15]These authors contributed equally to this work
[16]Present address: Weill Cornell Medical College, New York, NY 10021, USA
[17]Present address: University of Texas Health Science Center, San Antonio, TX 78229, USA
[18]Present address: Universidade Estadual de Campinas, Campinas, São Paulo 13083-970, Brazil
*Correspondence: bpaw@rics.bwh.harvard.edu
http://dx.doi.org/10.1016/j.ajhg.2013.09.011.

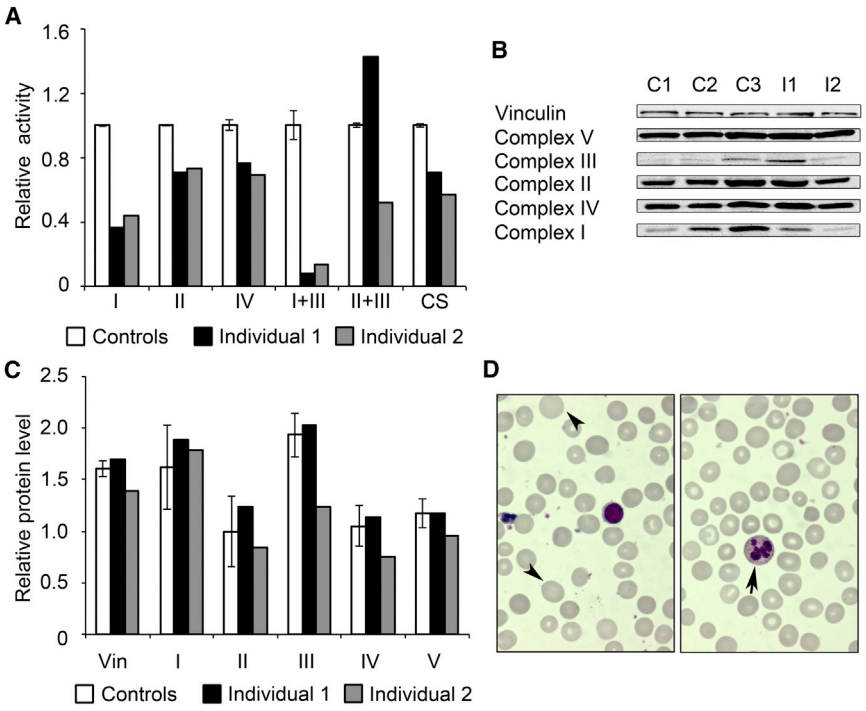

Figure 1. Individual 1 Has Macrocytic Anemia, and Both Individuals Present with Mitochondriopathy

(A) The RCA defect was seen in primary fibroblasts from both individuals, but not in control fibroblasts. RCA activity was assayed as described.[3] Error bars represent the SEM.

(B) Immunoblot analyses of mitochondrial-respiratory-complex proteins from control fibroblasts (C1, C2, and C3) and fibroblasts from the two affected individuals (I1 and I2) are displayed.

(C) Densitometric quantification of the respiratory-complex proteins, shown in (B), demonstrates intact expression of the respiratory-chain components. Error bars represent the SEM.

(D) Peripheral-blood smears from individual 1 reveal erythroid macrocytosis (left, arrow heads) and hypersegmented neutrophils (right, arrow).

Individual 2 is a 6-year-old girl of European origin and was born to nonconsanguineous German parents at 37 weeks of gestation. Similar to the delivery of individual 1, the delivery of individual 2 was induced because of IUGR. Weight, length, and cranial circumference were initially at the third percentile until she reached the age of 18 months, when she recovered normal height and weight. From birth, she had elevated lactate concentrations in blood and cerebrospinal fluid, which improved with a ketogenic diet. Muscle biopsy at 1 year of age revealed significantly reduced complex I activity (Table S1). She has severe visual deficit with delayed bilateral visual-evoked potential, but electroencephalography, nerve conduction studies, and auditory-evoked potential were normal. Although her gross motor skills are almost normal, she continues to show severe deficits in fine motor skills, visual-motor integration, and coordination. Erythrocyte mean corpuscular volume has always been in the upper range of normal without elevated methylmalonic acid excretion (Table S2). She regularly receives carnitine, a mixture of essential micronutrients, coenzyme Q_{10}, and riboflavin.

In summary, both individuals share a similar clinical presentation consistent with mitochondrial disease: IUGR, microcephaly, hypotonia, vision impairment, speech delay, and lactic acidosis due to a severe and consistent reduction in RCA (Figure 1A). Generalized defects in the expression of the mitochondrial respiratory complexes and mitochondrial mass were excluded by immunoblot analysis (Figures 1B and 1C).

For individual 1, blood measurements revealed decreased red blood cell counts. Red blood cell size was highly variable, and the average was larger than normal (Table S2). Also consistent with megaloblastic maturation, peripheral-blood smears revealed hypersegmented neutrophils (Figure 1D). Individual 2 exhibited milder erythroid abnormalities; her red blood cell size was highly variable but within normal limits. Metabolites associated with macrocytosis were within the normal range for both individuals (Table S2). White blood cell indices and platelet counts were also normal (data not shown).

The erythroid abnormalities from individual 1 cannot be explained by known mechanisms. All known causes of macrocytosis were excluded. Reticulocyte count was not indicated because her peripheral-blood smear did not reveal elevated polychromasia, spherocytes, schistocytes, or nucleated red blood cells. She also showed normal liver function, and therefore, liver-disease-associated abnormal lipid metabolism could be excluded. This individual had normal thyroid-function test results. Additionally, individual 1 had normal white blood cell and platelet counts, so bone marrow diseases (myelodysplastic syndrome, acute leukemia) were excluded. Furthermore, the individual had no exposure to alcohol, toxins, or drugs that induce macrocytic anemia (substances reviewed by Aslinia et al.).[2] Bone marrow aspiration and biopsy were not performed because they would cause significant pain and discomfort without a clear therapeutic or diagnostic benefit, a decision concurred by the local human subjects institutional review board in Italy. We further excluded known causes of megaloblastosis from vitamin deficiency and disorders of transport and absorption, such as pernicious anemia (MIM 170900) and Imerslund-Gräsbeck syndrome (MIM 261100) given that individual 1 had normal serum B_{12} and folate.[4,5] Rare diseases, such as transcobalamin II deficiency (MIM 275350) and defects in cellular cobalamin modification, are also known to

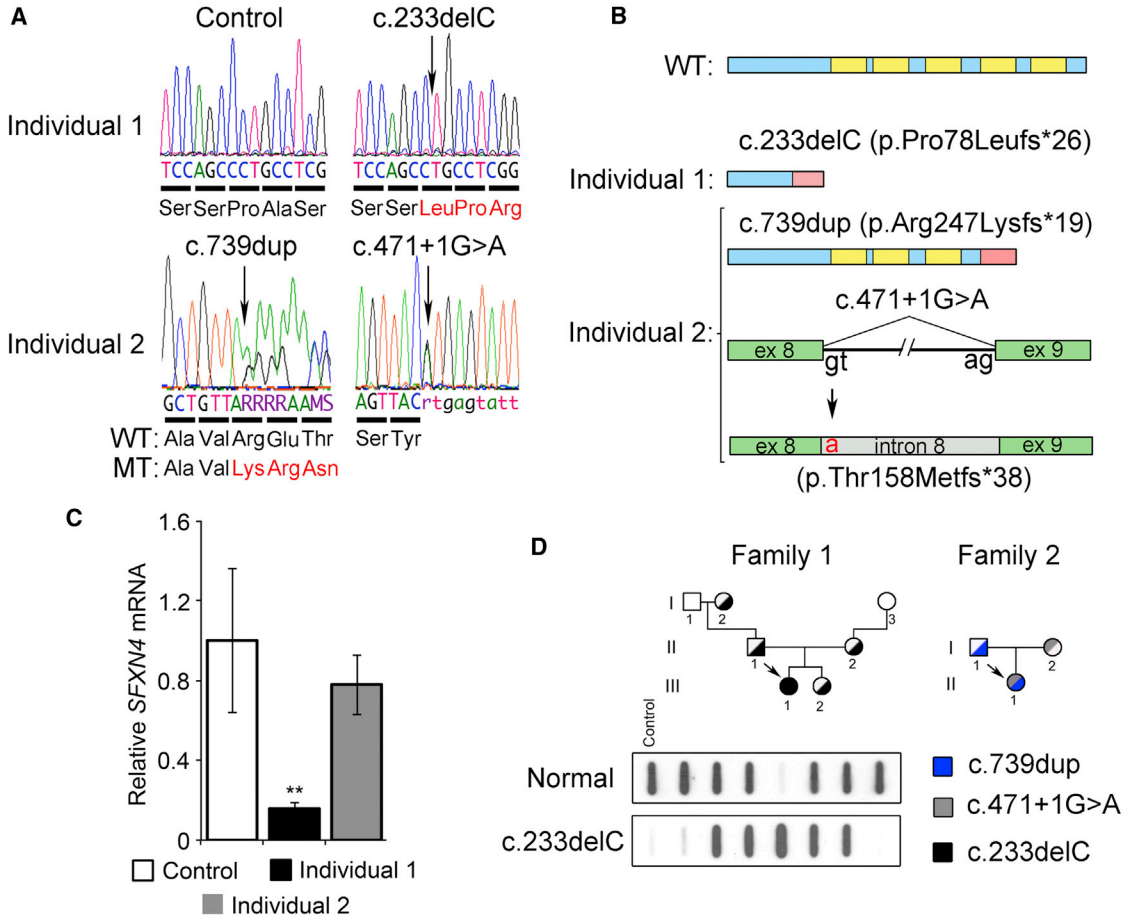

Figure 2. Next-Generation Sequencing Identifies Mutations in *SFXN4*

(A) Upper panel: sequencing revealed a single-nucleotide deletion (c.233delC) in the *SFXN4* cDNA from individual 1 (right), but not in the control (left). Lower panel: sequencing of individual 2 revealed two mutations, c.739dup (left) and c.471+1G>A (right). The normal and aberrant amino acid sequences are displayed below each chromatogram.

(B) A schematic representation of the normal SFXN4 is shown with the predicted multispanning transmembrane domains (top, highlighted in yellow). The c.233delC mutation in individual 1 results in a frameshift (highlighted in pink) and an eventual nonsense substitution at amino acid residue 102 (p.Pro78Leufs*26). In individual 2, the c.739dup mutation also causes a frameshift (pink) and premature termination at amino acid 266 (p.Arg247Lysfs*19), whereas the c.471+1G>A mutation affects the splice donor site at intron 8, causes its retention in the misspliced mRNA, and thus results in the insertion of an additional 38 amino acids after Tyr157 (p.Thr158Metfs*38).

(C) qRT-PCR analysis from control and affected fibroblasts revealed decreased steady-state *SFXN*4 mRNA when normalized to glyceraldehyde-3-phosphate dehydrogenase (*GAPDH*), correlating the disease severity with the residual *SFXN4* mRNA level; **$p < 0.0005$. qRT-PCR was performed with TaqMan probes for *SFXN4* and *GAPDH* (Applied Biosystems, Life Technologies). *SFXN4* expression was analyzed with the standard curve method, and *GAPDH* was used as a normalization control. Error bars represent the SEM.

(D) Family 1: Mendelian recessive-inheritance segregation was demonstrated in the family of individual 1 (arrow, III-1) by allele-specific oligonucleotide hybridization with the normal (top) or mutant c.233delC (bottom) ^{32}P-labeled probes. The control is a GM00536A healthy male. Family 2: the compound heterozygosity of individual 2 (arrow, II-2) was established with Sanger dideoxy sequencing.

cause megaloblastic anemia in individuals with normal serum B_{12} and folate but elevated homocysteine and/or methylmalonic acid.[4,5] Importantly, individual 1 had normal levels of metabolic intermediates, thereby ruling out defects in this canonical pathway. Orotic aciduria (MIM 258900) also causes megaloblastic anemia, but this too was excluded because both individuals showed no detectable levels of orotic acid in their urine (data not shown).[6] We propose that individual 1 has a hitherto uncharacterized macrocytic erythroid abnormality.

With the approval of the human subjects ethics committees from the University of Florence and the Technical University of Munich and the informed consent of the affected individuals' parents, we proceeded to study the genetic basis of this disease. We used the coexistent mitochondrial disease from individual 1 to narrow the range of potential candidates to mitochondrial genes or nuclear genes encoding mitochondrial proteins.[7] With this targeted approach, we used next-generation sequencing (Illumina GA-II platform) to identify a mutation in individual 1 in the putative mitochondrial-protein-encoding gene sideroflexin 4 (*SFXN4* [RefSeq accession number NM_213649.1]).[7,8] In individual 1, we found a homozygous single-nucleotide deletion (c.233delC) in *SFXN4*

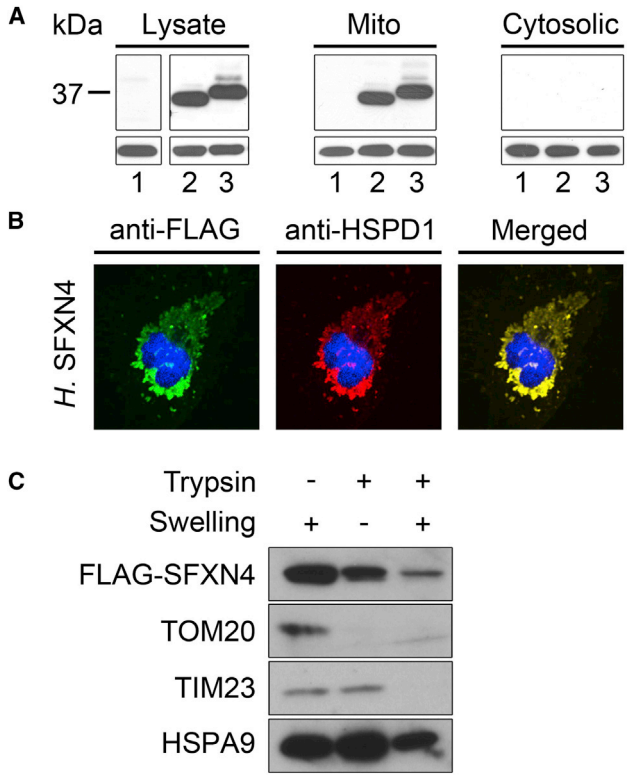

Figure 3. SFXN4 Localizes to the Inner Mitochondrial Membrane

(A) With the use of Lipofectamine 2000 (Invitrogen) and immunoblot analysis with FLAG antibody (Sigma) (lane 1, mock transfection; lane 2, zebrafish *sfxn4*; lane 3, human *SFXN4*), FLAG-tagged SFXN4 from human and zebrafish was found to localize to the mitochondria in transiently transfected Cos7 cells. Lysate refers to total cellular lysate, and mito (mitochondrial) and cytosolic refer to the subcellular fractions. HSPD1 (total and mitochondrial; Santa Cruz) and GAPDH (cytosolic; Santa Cruz) antibodies were used as loading controls. Cells were prepared for immunoblotting as previously described.[16] FLAG antibodies were obtained from Sigma. Goat anti-mouse IgG-HRP was used as a secondary antibody. Proteins were visualized with the SuperSignal West Pico Substrate chemiluminescent (Pierce).

(B) Confocal immunofluorescence microscopy confirmed the colocalization of FLAG-SFXN4 (FITC, green) with HSPD1 (Texas Red) (Pearson's correlation coefficient, 0.74), a mitochondria resident protein (yellow, merged panel). Nuclei were stained with DAPI (blue). The correlation between the signal from the FLAG-tagged SFXN4 and mitochondrial marker HSPD1 was calculated with software developed by Tony Collins, Wayne Rasband, and Kevin Baler. The Pearson's coefficient was compared against 74 randomized iterations of the HSPD1 images via the Fay method[17] and was statistically significant ($p < 0.05$). FITC and Texas-Red-conjugated secondary antibodies were obtained from Santa Cruz.

(C) FLAG-SFXN4 localized to the inner mitochondrial membrane in transfected HeLa cells after trypsin digestion (lane 2). TIM23, an inner-membrane protein, was protected from trypsin digestion, whereas TOM20, an outer-membrane protein, was degraded (lane 2). Rupturing of the mitochondrial inner membrane by hypotonic treatment showed that FLAG-SFXN4 and TIM23 were sensitive to proteolysis, whereas HSPA9, a matrix protein was protected (lane 3). The residual protease-resistant FLAG-SFXN4 reflects mitochondria that are resistant to osmotic shock. Proteins were detected with FLAG (Gilbertsville), TOM20 (Santa Cruz), TIM23 (BD Biosciences), and HSPA9 (Santa Cruz) antibodies.

(Figure 2A); it is predicted to introduce a frameshift and a premature stop codon prior to the region encoding all five predicted transmembrane domains (p.Pro78Leufs*26) (Figure 2B).

Exome sequencing (Illumina HiSeq2000 platform) in individual 2 identified heterozygous, predicted loss-of-function mutations in *SFXN4* (Figure 2A).[9,10] The first mutant allele, c.739dup, causes a frameshift and a premature truncation of the polypeptide before the two terminal transmembrane domains (p.Arg247Lysfs*19) (Figures 2A and 2B). The mutation in the second allele, c.471+1G>A, alters the canonical splice donor site, resulting in the insertion of intron 8 into the mature mRNA (Figure 2B). This intronic insertion in the open-reading frame predicts an additional 38 amino acids after Tyr157 and a subsequent premature translational termination (p.Thr158Metfs*38). The misspliced mRNA isoform also predicts that an internal alternate ATG/Met initiator at Met168 could allow translation of an in-frame polypeptide encoding the C-terminal portion of SFXN4 with potential partial activity.

To determine whether the gene was expressed, we assessed the steady-state level of *SFXN4* mRNA from the affected individuals' fibroblasts. Quantitative RT-PCR (qRT-PCR) showed that *SFXN4* expression was 84% lower in individual 1 but only 22% lower in individual 2 (Figure 2C) than in controls. The results for individual 1 are consistent with nonsense-mediated decay of the mutant transcript.[11] Taken together, these data suggest that the c.233delC mutation in individual 1 results in a severe loss-of-function phenotype. In contrast, the compound-heterozygous mutations in individual 2 are most likely hypomorphic, resulting in a higher residual level of *SFXN4* mRNA, which is consistent with her milder clinical course.

To establish the inheritance pattern of these mutations, we used allele-specific oligonucleotide hybridization and Sanger sequencing to genotype the affected individuals and their family members as previously described.[12–14] Normal DNA (control) was isolated from a lymphoblastoid line, GM00536A (Coriell Institute, Camden). The region surrounding the mutation was amplified via PCR with primers listed in Table S3. The results, summarized in Figure 2D, indicate that the mutant alleles were inherited in a Mendelian recessive manner. Individual 1 (III-1 from family 1) is homozygous for the c.233delC mutation, and individual 2 (II-1 from family 2) is a compound heterozygote for the c.739dup and c.471+1G>A mutations.

Previous large-scale proteomic analysis identified SFXN4 as a mitochondrial protein.[15] By probing cellular fractions by immunoblot and by confocal immunofluorescence microscopy, we experimentally confirmed that SFXN4 efficiently targets the mitochondria (Figures 3A and 3B). We next sought to determine the submitochondrial localization of SFXN4. We isolated mitochondria from HeLa cells expressing FLAG-SFXN4 and treated them

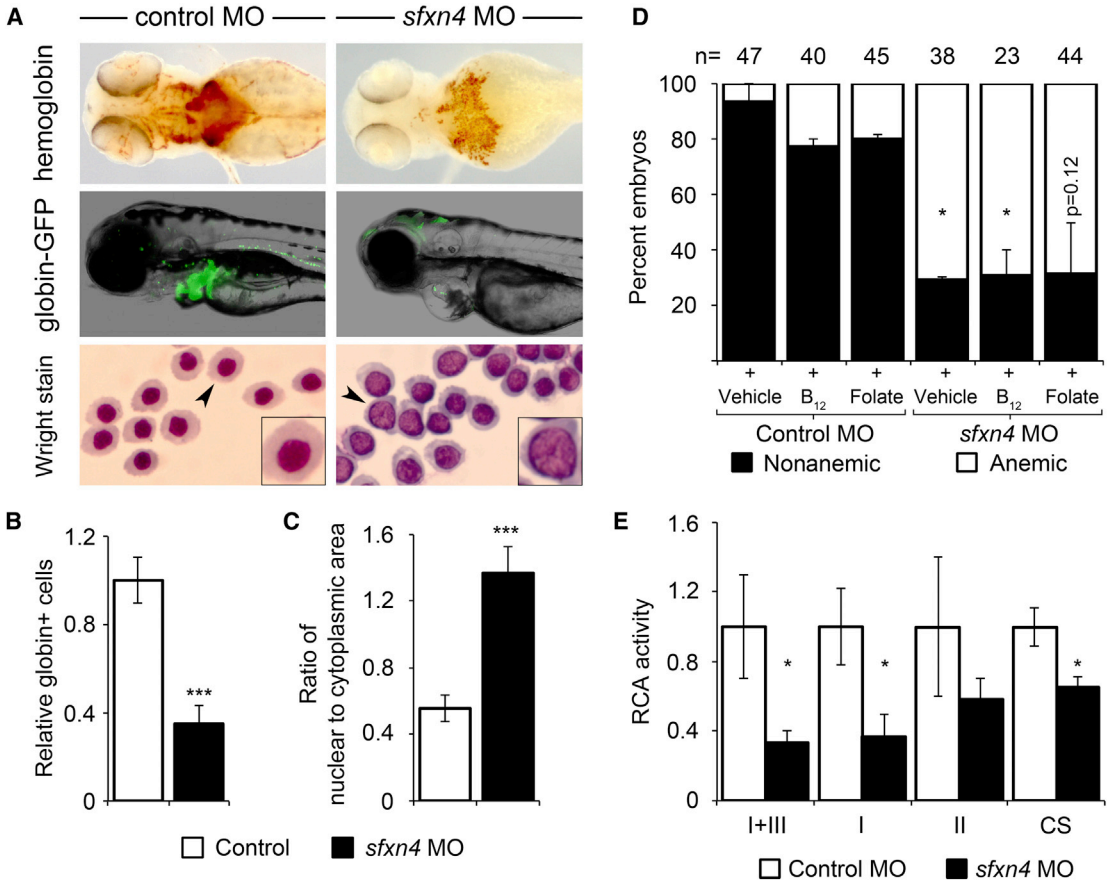

Figure 4. *sfxn4* Knockdown in Zebrafish Recapitulates the Defects in Erythropoiesis and Mitochondrial Respiration Seen in Individual 1
(A) Phenotypic characterization of control and zebrafish morphants for *sfxn4*. Zebrafish *sfxn4* morphants showed a defect in hemoglobinization (brown color) when stained with *o*-dianisidine (upper). The anemia in *sfxn4* morphants was evident by the reduction of GFP^+ erythroid cells in the *Tg(globin-LCR:eGFP)* transgenic zebrafish reporter line (middle). Cytospin analyses of flow-sorted erythroid cells from the control (left) and *sfxn4* morphant (right) revealed large nuclei with noncondensed chromatin in the latter (lower). Enlarged magnifications of individual cells (arrow) are shown in the insets.
(B) Flow cytometry of the *Tg(globin-LCR:eGFP)* transgenic line quantified the anemia in *sfxn4* morphants with a splice-blocking MO (***$p < 0.0005$). Cells were collected from 20–100 control or MO-injected embryos, disaggregated and passed sequentially through 70 and 40 μm cell strainers, washed in Hank's Balanced Salt Solution (HBSS) (Sigma), and pelleted by low-speed centrifugation. The cells were resuspended in a final buffer containing HBSS. Cells were sorted in a BD Biosciences FACSVantage SE machine as described.[20,21] Error bars represent the SEM.
(C) Enumeration of the ratio of nuclear area to cytoplasmic area showed a large increase in nuclear size relative to residual cytoplasmic area (***$p < 0.0005$; $n > 250$ cells were analyzed for each condition). Erythrocytes were sorted from embryos as previously described[20] and stained with Wright-Giemsa dye in a clinical hematology laboratory (Dana-Farber Cancer Institute, Boston). Cells were individually given a chromatic threshold for designating nuclear and cytoplasmic regions. The nuclear and cytoplasmic areas were measured in Image J (National Institutes of Health) with investigator-coded software.[22] Analysis was confirmed by manual inspection of all samples, and cellular components given improper thresholds were excluded from the analysis. Nuclear and cytoplasmic areas were averaged from a minimum of 250 cells (total) from four independent samples and divided for obtaining the ratio of nuclear area to cytoplasmic area.[23] Statistical significance was established with a one-tailed Student's t test for paired samples. Error bars represent the SEM.
(D) Neither vitamin B_{12} (1.0 mM) nor folate (0.01 mM) chemically complemented the anemia in *sfxn4* morphant zebrafish raised in vehicle media (standard balanced salt solution). The vehicle- and vitamin B_{12}-treated *sfxn4* morphants were significantly more anemic than the control morphant samples exposed to either vehicle or vitamin B_{12} (*$p < 0.05$). Similarly, compared to morphant controls exposed to folate, folate-treated *sfxn4* morphants were anemic ($p = 0.12$). Doses were selected on the basis of established literature and adjusted for preventing developmental and chemical toxicity.[24,25] At 96 hr postfertilization, embryos were stained for hemoglobinized cells with *o*-dianisidine (Sigma) as described.[26] Error bars represent the SEM.
(E) Zebrafish *sfxn4* morphants, but not embryos injected with a standard control MO, exhibited global mitochondrial-respiratory-chain defects (complexes I and III, complex I, complex II, citrate synthase[3,27]) (*$p < 0.05$). Error bars represent the SEM.

with trypsin to digest exposed membrane proteins as previously described.[18] SFXN4 was found to degrade concurrently with an inner membrane control, TIM23, indicating that SFXN4 localizes to the mitochondrial inner membrane (Figure 3C).

To functionally validate the causal relationship, we modeled the disease by knocking down the corresponding gene by using two different morpholinos (MOs) (Table S3) in zebrafish (*Danio rerio*), an excellent model system for studying human disease.[19] All zebrafish experiments

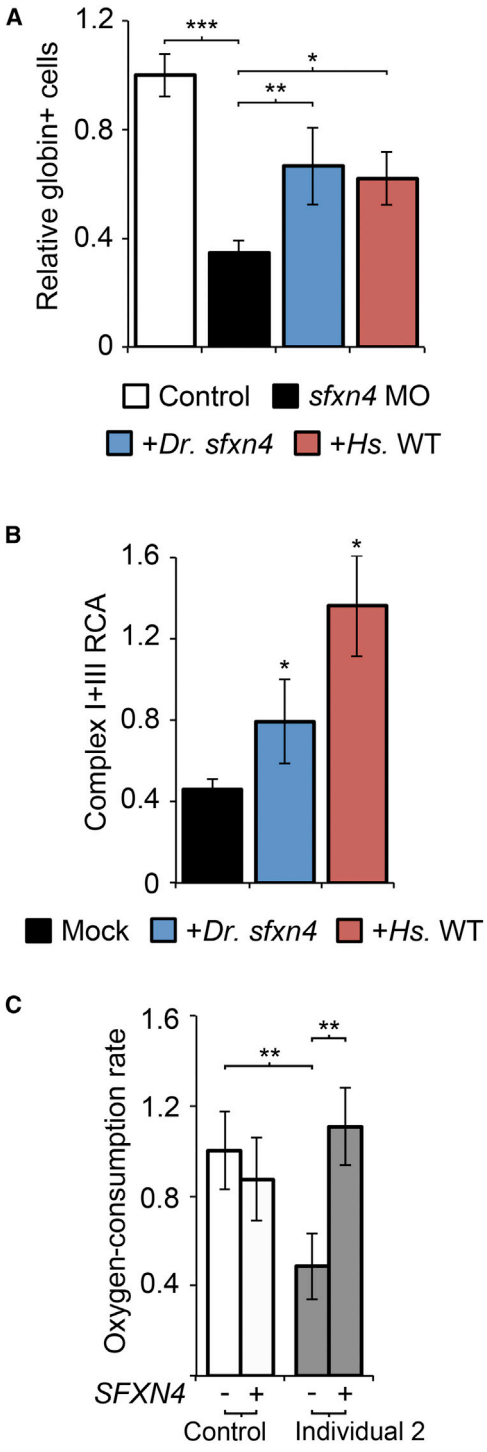

Figure 5. *SFXN4* Is Functionally Conserved across Vertebrate Species in Both Erythropoiesis and Mitochondrial Respiration
(A) Normal *SFXN4* cRNA from either zebrafish or human partially complemented the anemia in *sfxn4* morphant embryos (**p < 0.005, *p < 0.05). Zebrafish and human *FLAG-SFXN4* cDNA constructs in pXT7 were used for generating 5′ capped mRNA with the use of the mMessage mMachine T7 Kit (Ambion). The generated mRNA was mixed with MO at an equimolar concentration to the MO injection and injected at the 1-cell stage. The translational expression of the transgenic mRNA was confirmed by immunoblot analysis with FLAG antisera.
(B) Normal *SFXN4* cDNA from zebrafish and human complemented the RCA defect in primary fibroblasts of individual 1 (*p < 0.05). RCA for complexes I and III were compared to a mock-transfected (empty-vector) sample. Transfections were carried out with 5 μg of human or zebrafish *SFXN4* cDNA or empty vector pCS2+ with the use of Lipofectamine 2000 (Invitrogen).
(C) Lentiviral transduction of individuals 2's fibroblasts (performed as described[32]) with *SFXN4* cDNA (DNASU Plasmid Repository, clone ID HsCD00352377) cloned into the pLenti6/3/V5-TOPO vector system (Invitrogen) complemented the complex I respiratory deficiency. The oxygen-consumption rate was measured as previously described[10] after nontransduction (−) or *SFXN4* stable transduction with lentivirus (+) on fibroblasts from the control and individual 2 (**p < 0.01).
Error bars represent the SEM.

were conducted with the guidance and approval of the Institutional Animal Care and Use Committee at Boston Children's Hospital. By qRT-PCR, we confirmed the efficient knockdown of *sfxn4* (RefSeq NM_001076662) by both MOs (Figures S1A and S1B). MO-mediated knockdown of *sfxn4* in zebrafish embryos caused a gross reduction in hemoglobinized cells, as indicated by *o*-dianisidine staining (Figure 4A, upper panel). To quantify this reduction, we knocked down *sfxn4* in transgenic *Tg(globin-LCR:eGFP)* zebrafish, which express a GFP reporter under the regulation of the *globin-LCR* enhancer[28] (Figure 4A, middle panel). Fluorescence-activated cell sorting (FACS) analysis[20,21] revealed that relative to controls, *sfxn4* morphants had a 65% reduction of GFP^+ red blood cells (MO1: Figure 4B; MO2: Figure S1C). Additionally, *sfxn4* morphant embryos exhibited erythrocytes with enlarged nuclei containing open chromatin (mature teleost erythrocytes are nucleated), consistent with maturation arrest (Figure 4A, lower panel). Quantification of the nuclear/cytoplasmic ratio[22,23] showed that relative to control cells, red blood cells from *sfxn4* morphant fish exhibited a nearly 3-fold increase (Figure 4C). Interestingly, neither exogenous folate nor vitamin B_{12} supplementation could rescue the anemia seen in *sfxn4* morphants (Figure 4D). With our model system, these data experimentally validate the clinical findings that macrocytic anemia is independent of vitamin B_{12} and folate. *N*-acetylcysteine, a strong thiol antioxidant,[29–31] was also unable to rescue the anemia in *sfxn4* morphants, confirming that the anemia phenotype is not due to oxidative damage by reactive oxygen species (Figure S1D). Like the described affected individuals (Figure 1A), *sfxn4* morphants had global RCA defects (Figures 4E). In summary, *sfxn4* morphants recapitulated both the erythroid abnormality characterized in individual 1 and the mitochondrial respiratory defects observed in both individuals.

We validated the functional orthology of vertebrate *SFXN4* by using a combination of zebrafish and fibroblast complementation experiments. Relative to embryos injected with *sfxn4* MO alone, zebrafish embryos coinjected with *sfxn4* MO and either zebrafish or human *SFXN4* mRNA showed a significant increase in the erythrocyte population (Figure 5A). Using qRT-PCR, we confirmed the efficient knockdown of the endogenous *sfxn4* mRNA in the animals rescued with human *SFXN4* mRNA

(Figure S1A). Similarly, in fibroblasts from individual 1, the overexpression of both zebrafish and wild-type human *SFXN4* rescued the defect in the activity of complexes I and III without increasing the mitochondrial mass ($p < 0.05$) (Figure 5B). Furthermore, retroviral transduction of individual 2's fibroblasts, stably expressing human *SFXN4* cDNA, functionally complemented the mitochondrial RCA ($p < 0.01$) (Figure 5C). Together, these data describe pathologic mutations in *SFXN4* (c.233delC, c.739dup, and c.471+1G>A), demonstrate the functional conservation of SFXN4, and prove that the mutations are causative of both the mitochondrial and the erythroid pathologies observed in the individuals.

Hematologic manifestations of mitochondrial diseases are not unprecedented and include aplastic, macrocytic, or sideroblastic anemia, leukopenia, neutropenia, thrombocytopenia, or pancytopenia. They can occur in either syndromic or nonsyndromic mitochondrial disorders.[33] Despite these precedents, the pathogenic mechanisms linking mitochondrial dysfunction and hematological manifestations are poorly understood. Iron-metabolism dysfunction could play a central role in the sideroblastic anemia of the myopathy, lactic acidosis, and sideroblastic anemia (MLASA) syndromes (MLASA1 [MIM 600462] and MLASA2 [MIM 613561], caused by mutations in *PUS1* and *YARS2*, respectively)[34] and in X-linked sideroblastic anemia (MIM 300751), due to defects in *ALAS2*,[27] whereas a toxic iron overload occurs in GRACILE syndrome (MIM 603358).[35] Additional examples of mitochondrial diseases with hematological manifestations have been recently reviewed (*GLRX5* [MIM 609588], *SLC19A2* [MIM 603941], *SLC25A38* [MIM 610819], *ABCB7* [MIM 301310], and mtDNA deletions).[27]

SFXN4 is part of a superfamily of genes encoding predicted mitochondrial transmembrane proteins, presumably transporters. The founding family member, *Sfxn1*, was first reported to be mutated in the *flexed-tail* mouse mutant with sideroblastic anemia.[36] However, others have subsequently reported that the defect in these mice is in the transcription-factor-encoding gene *Smad5* rather than in *Sfxn1*.[37] This controversy remains unresolved. There is in vitro information to suggest that *Sfxn5* (*BBG-TCC*) can function as a mitochondrial citrate exchanger.[38]

Although the mechanism of disease remains elusive, it is clear that mutations in *SFXN4* are rare. On the basis of allele frequency in the National Heart, Lung, and Blood Institute Exome Sequencing Project Exome Variant Server, there are no common nonsynonymous variants in *SFXN4*. Interestingly, genome-wide association studies have yet to link mutations in *SFXN4* with hematologic[39–41] or neurologic disease.[42,43]

The identification of these rare mutations in *SFXN4* and their in vivo functional validation illustrate the power of coupling targeted exome sequencing with the zebrafish system for rapidly identifying and validating disease-causing mutations. Our studies demonstrate that SFXN4 should be added to the list of proteins required for mitochondrial homeostasis and hematopoiesis.

Supplemental Data

Supplemental Data include one figure and three tables and can be found with this article online at http://www.cell.com/AJHG.

Acknowledgments

We are indebted to the individuals described in our study and families for their participation. We thank members of our respective labs (Caiyong Chen and Jacky Chung) and Samuel E. Lux IV, H. Franklin Bunn, David G. Nathan, and Ellis J. Neufeld for critical feedback on the manuscript. We thank Leonard Zon for the *Tg(globin-LCR:eGFP)* transgenic line, Karin Hoffmeister for the use of the fluorescence-activated cell sorting machine, Caiyong Chen for protein technical advice, Ramiro Massol for confocal microscopy imaging, and Christian Lawrence and his team for the zebrafish husbandry. Fluorescence confocal microscopy was performed at the Harvard Digestive Disease Center Imaging Facility (Boston Children's Hospital). This work was supported by grants from the American Heart Association (J.D.C.), the American Society of Hematology (G.J.H.-S., J.D.C.), Cooley's Anemia Foundation (D.I.S.), the March of Dimes Foundation (6-FY09-289, B.H.P.), Coordenação de Aperfeicoamento de Pessoal de Nível Superior and Fundação de Amparo à Pesquisa do Estado de São Paulo (D.S.B.), GENOMIT (H.P.), the Marriott Mitochondrial Disorders Clinical Research Fund (V.K.M., S.D.), MEET (H.P.), MitoNET (H.P.), and the National Institutes of Health (K01 DK085217, D.I.S.; T32 HL007574 and F32 DK098866, Y.Y.Y.; R01 GM61721, C.M.K.; R01 GM097136, V.K.M.; P01 HD032062, S.D.M.; R01 DK070838 and P01 HL032262, B.H.P.).

Received: July 21, 2013
Revised: September 11, 2013
Accepted: September 18, 2013
Published: October 10, 2013

Web Resources

The URLs for data presented herein are as follows:

Colocalization Test, http://fiji.sc/Colocalization_Test
Image J, http://rsb.info.nih.gov/ij/
Online Mendelian Inheritance in Man (OMIM), http://www.omim.org
UniProt, http://www.uniprot.org/uniprot/Q6P4A7

References

1. Vafai, S.B., and Mootha, V.K. (2012). Mitochondrial disorders as windows into an ancient organelle. Nature *491*, 374–383.
2. Aslinia, F., Mazza, J.J., and Yale, S.H. (2006). Megaloblastic anemia and other causes of macrocytosis. Clin. Med. Res. *4*, 236–241.
3. DiMauro, S., Servidei, S., Zeviani, M., DiRocco, M., DeVivo, D.C., DiDonato, S., Uziel, G., Berry, K., Hoganson, G., Johnsen, S.D., et al. (1987). Cytochrome c oxidase deficiency in Leigh syndrome. Ann. Neurol. *22*, 498–506.
4. Yu, H.C., Sloan, J.L., Scharer, G., Brebner, A., Quintana, A.M., Achilly, N.P., Manoli, I., Coughlin, C.R., 2nd, Geiger, E.A.,

Schneck, U., et al. (2013). An X-linked cobalamin disorder caused by mutations in transcriptional coregulator HCFC1. Am. J. Hum. Genet. *93*, 506–514.

5. Gherasim, C., Lofgren, M., and Banerjee, R. (2013). Navigating the B(12) road: assimilation, delivery, and disorders of cobalamin. J. Biol. Chem. *288*, 13186–13193.
6. Nyhan, W.L. (2005). Disorders of purine and pyrimidine metabolism. Mol. Genet. Metab. *86*, 25–33.
7. Lieber, D.S., Calvo, S.E., Shanahan, K., Slate, N.G., Liu, S., Hershman, S.G., Gold, N.B., Chapman, B.A., Thorburn, D.R., Berry, G.T., et al. (2013). Targeted exome sequencing of suspected mitochondrial disorders. Neurology *80*, 1762–1770.
8. Calvo, S.E., Compton, A.G., Hershman, S.G., Lim, S.C., Lieber, D.S., Tucker, E.J., Laskowski, A., Garone, C., Liu, S., Jaffe, D.B., et al. (2012). Molecular diagnosis of infantile mitochondrial disease with targeted next-generation sequencing. Sci. Transl. Med. *4*, 18ra10.
9. Mayr, J.A., Haack, T.B., Graf, E., Zimmermann, F.A., Wieland, T., Haberberger, B., Superti-Furga, A., Kirschner, J., Steinmann, B., Baumgartner, M.R., et al. (2012). Lack of the mitochondrial protein acylglycerol kinase causes Sengers syndrome. Am. J. Hum. Genet. *90*, 314–320.
10. Haack, T.B., Haberberger, B., Frisch, E.M., Wieland, T., Iuso, A., Gorza, M., Strecker, V., Graf, E., Mayr, J.A., Herberg, U., et al. (2012). Molecular diagnosis in mitochondrial complex I deficiency using exome sequencing. J. Med. Genet. *49*, 277–283.
11. Isken, O., and Maquat, L.E. (2008). The multiple lives of NMD factors: balancing roles in gene and genome regulation. Nat. Rev. Genet. *9*, 699–712.
12. Paw, B.H., Tieu, P.T., Kaback, M.M., Lim, J., and Neufeld, E.F. (1990). Frequency of three Hex A mutant alleles among Jewish and non-Jewish carriers identified in a Tay-Sachs screening program. Am. J. Hum. Genet. *47*, 698–705.
13. Farr, C.J., Saiki, R.K., Erlich, H.A., McCormick, F., and Marshall, C.J. (1988). Analysis of RAS gene mutations in acute myeloid leukemia by polymerase chain reaction and oligonucleotide probes. Proc. Natl. Acad. Sci. USA *85*, 1629–1633.
14. Paw, B.H., Moskowitz, S.M., Uhrhammer, N., Wright, N., Kaback, M.M., and Neufeld, E.F. (1990). Juvenile GM2 gangliosidosis caused by substitution of histidine for arginine at position 499 or 504 of the alpha-subunit of beta-hexosaminidase. J. Biol. Chem. *265*, 9452–9457.
15. Pagliarini, D.J., Calvo, S.E., Chang, B., Sheth, S.A., Vafai, S.B., Ong, S.E., Walford, G.A., Sugiana, C., Boneh, A., Chen, W.K., et al. (2008). A mitochondrial protein compendium elucidates complex I disease biology. Cell *134*, 112–123.
16. Chen, W., Paradkar, P.N., Li, L., Pierce, E.L., Langer, N.B., Takahashi-Makise, N., Hyde, B.B., Shirihai, O.S., Ward, D.M., Kaplan, J., and Paw, B.H. (2009). Abcb10 physically interacts with mitoferrin-1 (Slc25a37) to enhance its stability and function in the erythroid mitochondria. Proc. Natl. Acad. Sci. USA *106*, 16263–16268.
17. Fay, F.S., Taneja, K.L., Shenoy, S., Lifshitz, L., and Singer, R.H. (1997). Quantitative digital analysis of diffuse and concentrated nuclear distributions of nascent transcripts, SC35 and poly(A). Exp. Cell Res. *231*, 27–37.
18. Chen, H.W., Rainey, R.N., Balatoni, C.E., Dawson, D.W., Troke, J.J., Wasiak, S., Hong, J.S., McBride, H.M., Koehler, C.M., Teitell, M.A., and French, S.W. (2006). Mammalian polynucleotide phosphorylase is an intermembrane space RNase that maintains mitochondrial homeostasis. Mol. Cell. Biol. *26*, 8475–8487.
19. Lieschke, G.J., and Currie, P.D. (2007). Animal models of human disease: zebrafish swim into view. Nat. Rev. Genet. *8*, 353–367.
20. Cooney, J.D., Hildick-Smith, G.J., Shafizadeh, E., McBride, P.F., Carroll, K.J., Anderson, H., Shaw, G.C., Tamplin, O.J., Branco, D.S., Dalton, A.J., et al. (2013). Teleost growth factor independence (gfi) genes differentially regulate successive waves of hematopoiesis. Dev. Biol. *373*, 431–441.
21. Amigo, J.D., Yu, M., Troadec, M.B., Gwynn, B., Cooney, J.D., Lambert, A.J., Chi, N.C., Weiss, M.J., Peters, L.L., Kaplan, J., et al. (2011). Identification of distal cis-regulatory elements at mouse mitoferrin loci using zebrafish transgenesis. Mol. Cell. Biol. *31*, 1344–1356.
22. Thon, J.N., Macleod, H., Begonja, A.J., Zhu, J., Lee, K.C., Mogilner, A., Hartwig, J.H., and Italiano, J.E., Jr. (2012). Microtubule and cortical forces determine platelet size during vascular platelet production. Nat Commun *3*, 852.
23. Pase, L., Layton, J.E., Kloosterman, W.P., Carradice, D., Waterhouse, P.M., and Lieschke, G.J. (2009). miR-451 regulates zebrafish erythroid maturation in vivo via its target gata2. Blood *113*, 1794–1804.
24. Zhao, Y., Qin, W., Zhang, J.P., Hu, Z.Y., Tong, J.W., Ding, C.B., Peng, Z.G., Zhao, L.X., Song, D.Q., and Jiang, J.D. (2013). HCV IRES-mediated core expression in zebrafish. PLoS ONE *8*, e56985.
25. Ma, Y., Wu, M., Li, D., Li, X.Q., Li, P., Zhao, J., Luo, M.N., Guo, C.L., Gao, X.B., Lu, C.L., and Ma, X. (2012). Embryonic developmental toxicity of selenite in zebrafish (Danio rerio) and prevention with folic acid. Food Chem. Toxicol. *50*, 2854–2863.
26. Amigo, J.D., Ackermann, G.E., Cope, J.J., Yu, M., Cooney, J.D., Ma, D., Langer, N.B., Shafizadeh, E., Shaw, G.C., Horsely, W., et al. (2009). The role and regulation of friend of GATA-1 (FOG-1) during blood development in the zebrafish. Blood *114*, 4654–4663.
27. Bergmann, A.K., Campagna, D.R., McLoughlin, E.M., Agarwal, S., Fleming, M.D., Bottomley, S.S., and Neufeld, E.J. (2010). Systematic molecular genetic analysis of congenital sideroblastic anemia: evidence for genetic heterogeneity and identification of novel mutations. Pediatr. Blood Cancer *54*, 273–278.
28. Ganis, J.J., Hsia, N., Trompouki, E., de Jong, J.L., DiBiase, A., Lambert, J.S., Jia, Z., Sabo, P.J., Weaver, M., Sandstrom, R., et al. (2012). Zebrafish globin switching occurs in two developmental stages and is controlled by the LCR. Dev. Biol. *366*, 185–194.
29. Yu, D., dos Santos, C.O., Zhao, G., Jiang, J., Amigo, J.D., Khandros, E., Dore, L.C., Yao, Y., D'Souza, J., Zhang, Z., et al. (2010). miR-451 protects against erythroid oxidant stress by repressing 14-3-3zeta. Genes Dev. *24*, 1620–1633.
30. Blanc, L., Ciciotte, S.L., Gwynn, B., Hildick-Smith, G.J., Pierce, E.L., Soltis, K.A., Cooney, J.D., Paw, B.H., and Peters, L.L. (2012). Critical function for the Ras-GTPase activating protein RASA3 in vertebrate erythropoiesis and megakaryopoiesis. Proc. Natl. Acad. Sci. USA *109*, 12099–12104.
31. Shah, D.I., Takahashi-Makise, N., Cooney, J.D., Li, L., Schultz, I.J., Pierce, E.L., Narla, A., Seguin, A., Hattangadi, S.M., Medlock, A.E., et al. (2012). Mitochondrial Atpif1 regulates haem synthesis in developing erythroblasts. Nature *491*, 608–612.

32. Kornblum, C., Nicholls, T.J., Haack, T.B., Schöler, S., Peeva, V., Danhauser, K., Hallmann, K., Zsurka, G., Rorbach, J., Iuso, A., et al. (2013). Loss-of-function mutations in MGME1 impair mtDNA replication and cause multisystemic mitochondrial disease. Nat. Genet. *45*, 214–219.
33. Finsterer, J. (2007). Hematological manifestations of primary mitochondrial disorders. Acta Haematol. *118*, 88–98.
34. Riley, L.G., Cooper, S., Hickey, P., Rudinger-Thirion, J., McKenzie, M., Compton, A., Lim, S.C., Thorburn, D., Ryan, M.T., Giegé, R., et al. (2010). Mutation of the mitochondrial tyrosyl-tRNA synthetase gene, YARS2, causes myopathy, lactic acidosis, and sideroblastic anemia—MLASA syndrome. Am. J. Hum. Genet. *87*, 52–59.
35. Fellman, V. (2002). The GRACILE syndrome, a neonatal lethal metabolic disorder with iron overload. Blood Cells Mol. Dis. *29*, 444–450.
36. Fleming, M.D., Campagna, D.R., Haslett, J.N., Trenor, C.C., 3rd, and Andrews, N.C. (2001). A mutation in a mitochondrial transmembrane protein is responsible for the pleiotropic hematological and skeletal phenotype of flexed-tail (f/f) mice. Genes Dev. *15*, 652–657.
37. Hegde, S., Lenox, L.E., Lariviere, A., Porayette, P., Perry, J.M., Yon, M., and Paulson, R.F. (2007). An intronic sequence mutated in flexed-tail mice regulates splicing of Smad5. Mamm. Genome *18*, 852–860.
38. Miyake, S., Yamashita, T., Taniguchi, M., Tamatani, M., Sato, K., and Tohyama, M. (2002). Identification and characterization of a novel mitochondrial tricarboxylate carrier. Biochem. Biophys. Res. Commun. *295*, 463–468.
39. Soranzo, N., Spector, T.D., Mangino, M., Kühnel, B., Rendon, A., Teumer, A., Willenborg, C., Wright, B., Chen, L., Li, M., et al. (2009). A genome-wide meta-analysis identifies 22 loci associated with eight hematological parameters in the HaemGen consortium. Nat. Genet. *41*, 1182–1190.
40. van der Harst, P., Zhang, W., Mateo Leach, I., Rendon, A., Verweij, N., Sehmi, J., Paul, D.S., Elling, U., Allayee, H., Li, X., et al. (2012). Seventy-five genetic loci influencing the human red blood cell. Nature *492*, 369–375.
41. Ganesh, S.K., Zakai, N.A., van Rooij, F.J., Soranzo, N., Smith, A.V., Nalls, M.A., Chen, M.H., Kottgen, A., Glazer, N.L., Dehghan, A., et al. (2009). Multiple loci influence erythrocyte phenotypes in the CHARGE Consortium. Nat. Genet. *41*, 1191–1198.
42. Foo, J.N., Liu, J.J., and Tan, E.K. (2012). Whole-genome and whole-exome sequencing in neurological diseases. Nat Rev Neurol *8*, 508–517.
43. Bras, J., Guerreiro, R., and Hardy, J. (2012). Use of next-generation sequencing and other whole-genome strategies to dissect neurological disease. Nat. Rev. Neurosci. *13*, 453–464.